Self-trapped exciton singlet–triplet splitting in crystals with α-quartz structure: SiO_2, SiO_2–Ge, GeO_2, $AlPO_4$ and $GaPO_4$

Self-trapped exciton singlet–triplet splitting in crystals with α-quartz structure: SiO$_2$, SiO$_2$–Ge, GeO$_2$, AlPO$_4$ and GaPO$_4$

A N Trukhin

University of Latvia, Solid State Physics Institute, LV-1063, Riga, Latvia

Abstract

A fast component of the self-trapped exciton (STE) luminescence was discovered in crystals with α-quartz structure such as SiO$_2$, SiO$_2$–Ge, GeO$_2$, AlPO$_4$ and GaPO$_4$, manifesting the singlet–singlet transitions of STEs. Comparison of time resolved photoluminescence (PL) spectra of triplet–singlet transitions and fast singlet–singlet transitions showed the singlet–triplet splitting of STEs in a pure SiO$_2$ α-quartz crystal to be 0.2 eV. In other crystals, the singlet–triplet splitting was found to be less than 0.2 eV. Small singlet–triplet intervals confirm that electrons of the STE are not confined in one atom's area.

(Some figures in this article are in colour only in the electronic version)

1. Introduction

The luminescence of pure crystalline quartz excited by ionizing radiation has been attributed to the self-trapped exciton (STE) in the papers of Griscom [1], Trukhin and Plaudis [2, 3]. The luminescence, situated at 2.6–2.7 eV [2] with a time constant of about 1 ms at 77 K, was ascribed to the triplet–singlet transition in STE. The latter was obtained with the approval of optically detected magnetic resonance (ODMR) [4] for the determination of the zero field split triplet state [5, 6]. Two types of STEs with similar structure but different orientations within the crystal structure were deduced. It was proposed that the existence of the two types of STEs is dictated by the α-quartz structure and was foreseen for the two types of STEs in crystals such as GeO$_2$, AlPO$_4$ and GaPO$_4$ with the α-quartz structure while only one type existed in other tetrahedral structured relevant materials such as cristobalite and coesite, and this was subsequently supported by experiments [7, 8].

The main tool used for the STE measurements was a pulsed electron gun, 20–10 ns duration at 250 kV [1, 3]. The cathodoexcitation experiment manifested transient absorption [1], whose spectrum resembled that of the non-bridging oxygen (NBO) and three-fold coordinated silicon (E'center) spectrum, initially seen in [1] and later in [9]. This represents the stepping stone of the STE model.

The model of STEs proposed in [10, 11] was based on the discovery of STEs near a germanium impurity in silicon dioxide α-quartz crystal and germanium dioxide crystal with α-quartz structure [7]. The decay time constant of photoluminescence (PL) was about 1 ms in the pure crystal, free of Ge doping. So, it was concluded that the spin–orbit interaction allowing transition from the triplet state was related to oxygen, with little dependence on silicon or germanium involved in the STE. Furthermore, the ODMR measurement [4] of the STE revealed a large value of the zero field splitting parameter, D_o (22 GHz), which was comparable to the D_o parameter of the molecular oxygen $\sim$60 GHz. So, the STE creation is related to the Si–O bond breaking or weakening and the formation of NBO, which relaxes and makes a bond with a bonding oxygen on the other side of the c or x, y channel. These two oxygen–oxygen bond orientations determine the orientation of the STE and the corresponding polarization of luminescence, as well as the different thermal stabilities of the two kinds of STEs. The two kinds of STEs are dictated by the oxygen–oxygen bond formation in crystals with α-quartz structure. We have observed two kinds of differently oriented STEs in the family of crystals with α-quartz structure such as GeO$_2$, AlPO$_4$ and GaPO$_4$ [7, 8]. In contrast, in coesite and cristobalite, the tetrahedral structured polymorph modifications of SiO$_2$, we have observed only one type of STE [3, 12]. The two types of STEs in these crystals are also
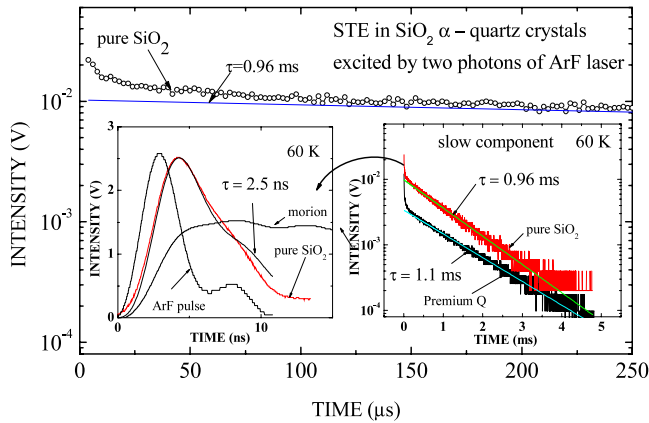
Figure 1. STE PL decay kinetics under two-photon ArF laser excitation of pure SiO$_2$ α-quartz for fast (left insertion) and slow (right insertion) components. The ArF laser pulse and synthetic Premium Q decay of PL are presented for comparison. The fit curve is obtained by convolution of an exponential decay with $\tau = 2.5$ ns and ArF laser pulse shape.

Figure 2. Time resolved PL spectra under two-photon ArF laser excitation of pure SiO$_2$ α-quartz for fast PL and slow PL as well as the corresponding spectral dependence of the time constant. $T = 80$ K.

determined by the α-quartz structure. This is reflected in the different luminescence polarizations of the slightly different luminescence bands, as well as in the different values of thermal quenching energies. The two types of STEs differing in orientation and quenching energies are clearly observed in the AlPO$_4$ and GaPO$_4$ crystals [8]. In h-GeO$_2$ the quenching energies are the same but the orientations are different, therefore the total degree of polarization in the GeO$_2$ α-quartz crystal is the lowest among the family of materials [7]. In all the studied cases, the two kinds of STEs differ in their polarizations, even though their temperature dependence is the same as in GeO$_2$. However, in the octahedral structured SiO$_2$ and GeO$_2$ with rutile structure (stishovite and argutite), we did not find similarities with the α-quartz STE [12].

Use of ArF and F$_2$ excimer lasers allows a more precise measurement of the parameters of STEs, as we have previously shown for the silicon dioxide pure crystal in the study of zero field splitting of the triplet state of STE created by a two-photon process [6]. In this study, the triplet–singlet splitting of the same electron configuration was performed.

The singlet–triplet splitting of STEs, a knowledge of which is essential for modeling, has not yet been studied for crystals with α-quartz structure due to experimental difficulties. A large value of the splitting corresponds to confinement of the STE within atomic dimensions [13, 14]. Excimer lasers and fast photomultiplier provide the basis for performing the search for singlet–singlet luminescence of STEs in the α-quartz structured crystals. Examples of such studies in other materials such as rare element and alkali halide crystals are reflected in detail in the monograph [13]. The physics of the singlet and triplet states is presented in detail in the monograph [14].

2. Experimental details

The samples used for the investigation were synthetic silicon dioxide α-quartz crystals, in the pure form previously studied
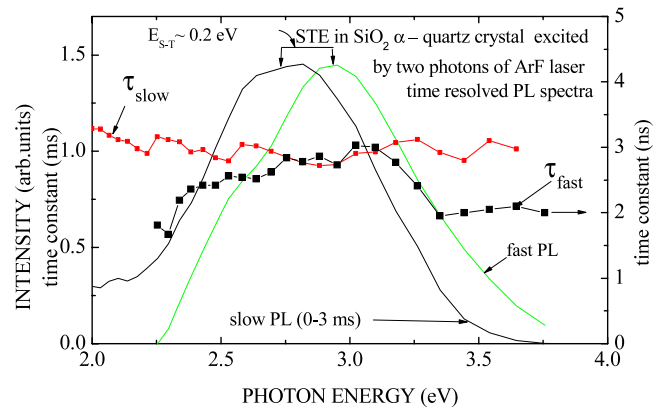
in [6] and activated with 0.1 wt% of Ge previously studied in [5]. These samples, 10 mm $\times$ 10 mm $\times$ 1 mm in dimension, were cut perpendicular to the optical axis. The other samples used were smaller crystals of GeO$_2$, AlPO$_4$ and GaPO$_4$, about 1 mm^3 in dimension, antecedently studied in [7, 8].

The F$_2$ laser (157 nm, model PSX-100, manufactured by Neweks, Estonia) produced 0.5 mJ, 5 ns pulses while an ArF laser (193 nm) of the same type was used with 10 times higher power. The shape of the pulses was used for the deconvolution of the measured fast curve of the samples PL. The F$_2$ laser light was passed through a copper tube with flowing nitrogen. A crystalline silicon dioxide crystal was used as a window to let in the light of the excitation lasers. A two-photon regime was achieved with a long focus lens (275 mm) made of silica glass, for ArF laser light. A cryostat maintained the temperature in the 60–350 K range. Luminescence was detected with a photomultiplier tube H6780-04 through a grating monochromator MCD-1. An oscilloscope (Textronic TDS 2022B) was exploited for the decay curve registration. The F$_2$ laser photon energy (7.9 eV) lies within the intrinsic absorption thresholds of GeO$_2$, AlPO$_4$ and GaPO$_4$, situated at 6, 7.9 and 7.3 eV respectively, as well as in the intra-center transitions of the SiO$_2$–Ge crystal. The crystals could then be excited via the single-photon process. The ArF laser (6.4 eV) allows the single-photon excitation regime only in GeO$_2$ while the other materials studied could be excited in the two-photon regime.

3. Results

The main data for pure silicon dioxide are presented in figures 1 and 2. The decay kinetics is composed of two components: a slow component with a time constant of about 1 ms (right insertion), as was known from previous experiments (see, for example [10, 11]) and a fast component (left insertion). An intermediate decay is also observed (the curve on the main part of figure 1). It could be ascribed to the previously studied, (see e.g. [15]) alkali related luminescence center, excited by the single-photon process.
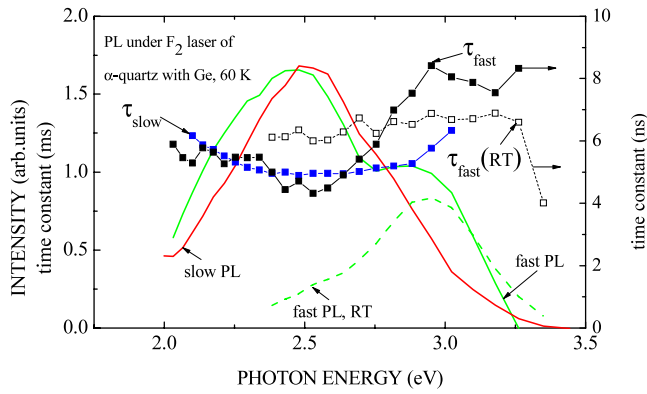
Figure 3. Time resolved PL spectra under F_2 laser excitation of germanium doped SiO_2 α-quartz for fast PL and slow PL as well as the corresponding spectral dependence of the time constant measured at $T = 80$ K. The '$\tau_{fast}(RT)$' and the 'fast PL, RT' presents spectral dependence of fast PL and the time constant at 290 K.
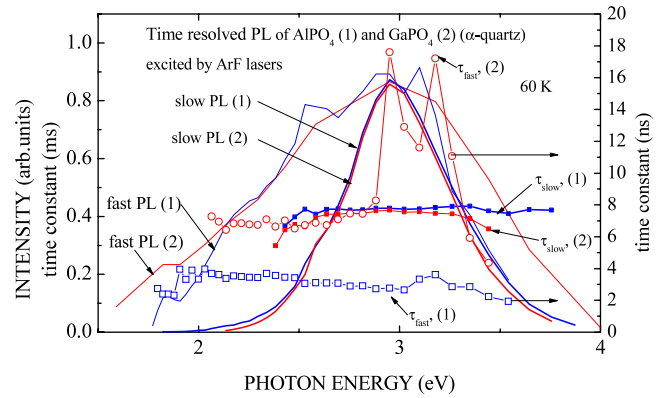

Figure 5. Time resolved PL spectra under two-photon ArF laser excitation of $AlPO_4$ (1) and $GaPO_4$ (2) α-quartz for fast PL and slow PL as well as the corresponding spectral dependence of the time constant. $T = 60$ K.
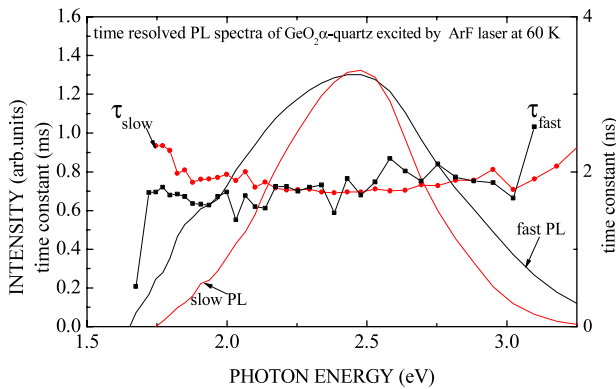

Figure 4. Time resolved PL spectra under ArF laser excitation of GeO_2 α-quartz for fast PL and slow PL as well as the corresponding spectral dependence of the time constant. $T = 60$ K.
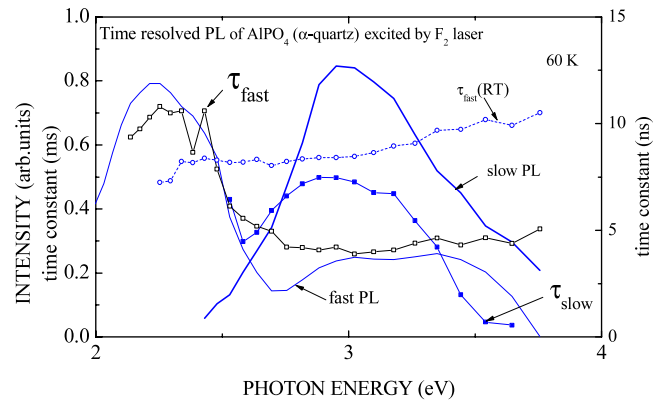

Figure 6. Time resolved PL spectra under F_2 laser excitation of $AlPO_4$ α-quartz for fast PL and slow PL as well as the corresponding spectral dependence of the time constant. $T = 60$ K.

A mutual proportionality between the fast and the slow components of decay is observed. The higher the intensity of the slow luminescence, the greater the fast component of decay. It is possible to estimate the decay time constant for the fast component by selection of the exponential decay curve convoluted with the shape of the laser pulse. The best selected exponent is one with a time constant of 2.5 ns, for the left insertion of figure 1. The deviation between the measured and the convoluted curves determines the precision of measurements under conditions of stray current induced by laser discharge.

The spectral dependences shown in figure 2, for the fast and the slow component of luminescence are different. The slow PL band is situated at 2.7 eV, having a FWHM equal to 0.81 eV, as is the case for STE in pure α-quartz and the fast PL band is situated at 2.9 eV with FWHM equal to 0.81 eV. The maximum of the fast luminescence band is shifted towards higher energy by 0.2 eV. The intensity of luminescence is obtained by the integration of the decay curves of each point in the spectra. The broad PL band has an average decay time constant of 1 ± 0.1 ms, practically independent of its position in the spectrum and in good agreement with the previous

data [1–6]. The fast component of decay has a slight deviation of 2–3 ns, within the PL band. The precision of the fast time constant determination is about 30%.

In the case of SiO_2–Ge, GeO_2, $AlPO_4$ and $GaPO_4$ crystals, the fast component of the decay is observed for both F_2 and ArF laser excitations as well as an intermediate component. The latter is explained by the role of luminescence unrelated to the intra-center transition in STE. The corresponding figures with the kinetics are very similar to that of figure 1, and are not discussed in this paper. The spectral parameters are presented in figures 3–6. Let us consider them separately.

In the case of SiO_2–Ge, the slow PL band is situated at 2.5 eV, having a FWHM equal to 0.69 eV, as is the case for STE near a Ge impurity in this crystal, shown in figure 3. The decay time constant for the slow PL is about 1 ms, and is in good agreement with the previous measurements [5, 16]. The fast PL contains two sub-bands: one at 2.47 eV and another at 2.9 eV. At room temperature, the band at 2.47 eV is strongly quenched and only the 2.9 eV band remains. The band at 2.9 eV may correspond to the fast band in a pure silicon dioxide α-quartz crystal. The time constant varies between 5–8 ns within these two sub-bands for the low temperature Ge doped crystal. At

room temperature, the decay time constant, equal to 7 ns of the remaining sub-band at 2.9 eV, is stable within the band and is consistent with the time constant in a pure SiO_2 crystal at RT. The fast PL band at 2.47 eV agrees well with the slow PL band. The disappearance of the green band during laser irradiation correlates with the radiation properties of SiO_2–Ge [17].

In the case of a GeO_2 crystal with α-quartz structure, the fast and the slow PL bands are similarly situated at 2.47 eV, as shown in figure 4 and the corresponding FWHMs are 0.60 and 0.87 eV for the slow and the fast band respectively. The decay time constant of the slow band is 0.8 ms, in good agreement with the previous data [7] and 2 ns for the fast PL corresponding to its band maximum. The time constants for both decay components are practically independent within the PL bands. The data are very similar for both the ArF and F_2 lasers.

In the cases of $AlPO_4$ and $GaPO_4$, there are some differences between the data from ArF and F_2 lasers. In the ArF two-photon excitation, the slow PL band is situated at 2.95 eV for both the crystals, as shown in figure 5 and the FWHM are 0.61 and 0.58 eV for $AlPO_4$ and $GaPO_4$ respectively. The fast PL bands are also similar, with the maxima situated at 2.95 eV, although with distorted band shapes and the FWHM estimated at 0.95 and 1.14 eV for $AlPO_4$ and $GaPO_4$ respectively. The decay time constants of the slow components are practically coincidental in both materials for ArF laser excitation and lower than in the previous measurement [8]. This decay constant of 0.4 ms is independent of the position of the slow PL band. The fast component time constant for $AlPO_4$ is about 4–2 ns and decreases towards the UV part of the PL band while that of $GaPO_4$ is higher and equal to 7 ns in the range of 2–2.9 eV with an increase of up to 17 ns in the range of 3–3.4 eV. The latter could be related to some uncontrolled impurities obscuring the decay of the STE, due to excitation of the impurity in a single-photon process by the ArF laser.

In the case of the F_2 laser, the data for both materials differ significantly, as shown in figures 6 and 7. The slow PL band is situated at 2.98 eV for $AlPO_4$ (figure 6) and 2.95 eV for $GaPO_4$ (figure 7). The corresponding bandwidths are 0.73 and 0.56 eV respectively. The fast PL band for $GaPO_4$ consists of a single band at 2.95 eV with FWHM equal to 0.62 eV, however, that of $AlPO_4$ is complicated and contains at least three sub-bands at 2.2, 3 and 3.4 eV, respectively. The slow decay time constants are not similar for the two materials as was observed in the two-photon ArF laser excitations. It is about 0.5 ms at the band maximum, though significantly declining towards the wings of the band in the case of $AlPO_4$. For $GaPO_4$, the slow time constants are about 0.5 ms at 60 K and 0.3 ms at 80 K, slightly varying within the PL band, as in figure 7. The differences in the slow decay for 60 and 80 K reflect the two stages of STE in $GaPO_4$ and agree with the data in [8]. The fast time constant values are approximately 4 and 3 ns for $AlPO_4$ and $GaPO_4$ respectively, with small changes within the PL band. In both cases, the fast time constant almost doubles at room temperature—this effect was observed for SiO_2 pure crystal. The F_2 laser photon energy falls within the intrinsic absorption of the $GaPO_4$, hence both laser cases are similar
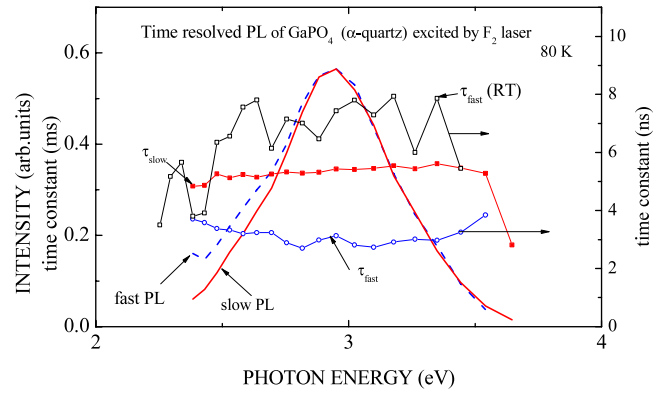

Figure 7. Time resolved PL spectra under F_2 laser excitation of $GaPO_4$ α-quartz for fast PL and slow PL as well as the corresponding spectral dependence of the time constant. $T = 80$ K. τ_{fast}(RT) presents the spectral dependence of the fast time constant at 290 K.

because only the intrinsic states are excited. In the case of $AlPO_4$, the photon energy of the F_2 laser corresponds to the low energy tail of the intrinsic absorption. Therefore, single-photon excitation of defect states, usually taking place within the range of a material, is very probable. Indeed, the fast PL sub-band at 2.2 eV possesses a noticeably different decay from the sub-bands at 3 and 3.4 eV, as in figure 6. This sub-band is not resolved for ArF laser excitation.

4. Discussion

The fast and slow components of PL decay were observed in crystals with α-quartz structure such as SiO_2, SiO_2–Ge, GeO_2, $AlPO_4$ and $GaPO_4$ using ArF and F_2 lasers pulses. The time resolved slow PL bands and the values of the decay time constants correspond well with the known parameters of STE of the triplet–singlet luminescence in those materials [18]. Furthermore, the temperature dependences of the time resolved PL intensity and time constant (not discussed in this paper) exhibit two stages of thermal quenching, characteristic of the α-quartz crystals. So, the STEs are created under the influence of laser pulses in the studied materials. The fast time resolved PL bands correlate with that of the slow component and the observed fast component belongs to STE. The fast component of STE decay in the studied crystals with α-quartz structure corresponds to the singlet state of STEs. Hence, these data allow the determination of the singlet–triplet splitting or interval. In the case of pure silicon dioxide α-quartz, the splitting of 0.2 eV, could be estimated directly from the difference between the fast and the slow components of STE in the PL spectra, shown in figure 2. This value is twice as high as that of the rare crystal ($\sim$0.08 eV) but much smaller than in many alkali halides (1–2 eV) [13]. On the other hand, upon comparison with the known values of the singlet–triplet interval in other materials [14] we can conclude that STE in silicon dioxide stands for charge transfer transition, where the exchange interaction is small. In the cases of other studied materials, there is no possibility of such a clear determination of the splitting value. The values of FWHM for fast and slow PL in pure silicon dioxide are the same, whereas in the other

materials under study, the value is much higher for the fast component, and the maxima of the fast and slow PL bands are quite close to each other. The value of the singlet–triplet interval is much lower in these crystals than in silicon dioxide. The determination of these values requires further experiments and theoretical calculations.

The singlet–triplet splitting of one electronic configuration is determined only from the electrostatic repulsion of the electron or the exchange energy. Therefore, the small value of the singlet–triplet splitting for STEs in the crystal with α-quartz structure is determined by the large dimension of the STEs. This is consistent with the above proposed model, where one electron is in the antibonding state of the oxygen molecule and another electron in a diffused state of silicon.

The performed studies of the singlet state of STEs are in the initial stages and require experimental investigations of the decay kinetics using sharper pulses than that provided by the excimer ArF and F_2 lasers.

Further, theoretical calculations of both the slow and the fast decay time constants as well as the singlet–triplet splitting of the same electron configuration, and not only the singlet of the ground state of the crystal and the lowest energy triplet state of STEs, are needed along with experimental data and *ab initio* calculations. Existing calculations of the self-trapped exciton in the crystal with α-quartz structure do not provide these data. In silicon dioxide α-quartz crystal, many types of differently relaxed excitons are observed experimentally [10] besides the STEs. The performed calculations for STEs [19, 20] resemble those of the relaxed excitons rather than STEs with deep lattice relaxation.

Acknowledgments

References

[1] Griscom D L 1979 *32nd Freq. Control Symp. Electr. Indust Assn. (W-DC)* p 98
[2] Trukhin A and Plaudis A 1978 *4th Conf. on Radiation Phys. Chem. Ionic Crystals* (Rīga: University of Latvia) p 337
[3] Trukhin A N and Plaudis A E 1979 *Fiz. Tverd. Tela (Sov. Solid State Phys.)* **21** 1109
[4] Hayes W, Kane M J, Salminen O, Wood R L and Doherty S P 1984 *J. Phys. C: Solid State Phys.* **17** 2943
[5] Trukhin A N 1987 *Phys. Status Solidi* b **142** K83
[6] Trukhin A N, Kink M, Maksimov J and Kink R 2003 *Solid State Commun.* **127** 655
[7] Trukhin A N 1993 *Solid State Commun.* **85** 723
[8] Trukhin A N 1994 *Solid State Commun.* **90** 795
[9] Itoh C, Tanimura K and Itoh N 1988 *J. Phys. C: Solid State Phys.* **21** 4693
[10] Trukhin A N 1992 *J. Non-Cryst. Solids* **149** 32
[11] Trukhin A N 2000 *International School of Solid State Physics, 17th Course* (*NATO Science Series. II Mathematics, Physics and Chemistry Defects in SiO_2 and Related Dielectrics: Science and Technology* vol 2) ed D Griscom, G Pacchioni and L Skuja (Dordrecht: Kluwer) pp 235–83
[12] Trukhin A N, Jansons J L, Dyuzheva T I, Lityagina L M and Bendeliani N A 2003 *Solid State Commun.* **127/6** 415
[13] Song K S and Williams R T 1992 *Self-Trapped Excitons* (London: Springer)
[14] McGlynn S P, Azumi T and Kinoshita M 1969 *Molecular Spectroscopy of the Triplet State* (Englewood Cliffs, NJ: Prentice-Hall)
[15] Trukhin A N 1994 *J. Nucl. Instrum. Methods Phys. Res.* B **91** 334
[16] Trukhin A N, Baumanis E and Plaudis A E 1981 *Abstract IC Defects in Insulating Crystal* (Rīga: Zinātne) p 321
[17] Isoya J, Weil J A and Claridge R F C 1978 *J. Chem. Phys.* **69** 4876
[18] Trukhin A N 1996 *Proc. 13th Int. Conf. on Defect in Insulating Crystals*; *Mater. Sci. Forum* **239–241** 531
[19] Shluger A L and Stefanovich E 1990 *Phys. Rev.* B **42** 9664
[20] Van Ginhoven R M, Jonsson H, Peterson K A, Duouis M and Corrales L R 2003 *J. Chem. Phys.* **118** 6582